

CFD MODELING OF REAL SCALE SLAB REHEATING FURNACE

Hosain M.L.^{*,1,2} Bel Fdhila, R.^{1,2} Sand U.² Engdahl J.³ Dahlquist E.¹ Li H.¹

*Author for correspondence

¹Department of Energy, Building and Environment; School of Business, Society and Engineering,
Mälardalen University, Sweden

²ABB Corporate Research, Sweden

³SSAB, Borlänge, Sweden

E-mail: md.lokman.hosain@mdh.se

ABSTRACT

Understanding the complex transient flow and heat transfer characteristics inside the furnace is a precondition to optimize furnace operation while maintaining high standard steel products. In the industrial furnaces often hot spots have been observed inside the slabs due to the current alignment of the burners. The control of the slab heating uses surface temperature as boundary condition, and it is thus important to predict this as accurate as possible. Transient flow behavior and interactions between the burners make it challenging to find an optimal burner arrangement. However, Computational Fluid Dynamics (CFD) is one of the robust methods which can be used to simulate the flow and perceive the complexity in combustion and radiation associated with the furnace. The scope of this work is to simulate the slab reheating furnace to understand the flow pattern and provide the results as input to simplified zonal radiation method to use it in online control system in real plant. In this paper we present the CFD simulation results for a real scale slab reheating furnace in 3D and compare them with measurements. The simulation predicts the gas temperature similar to the measurement points. However, the slab surface and average temperature deviate from continuous curve generated from the interpolation based on measurements from few thermocouples. The flow pattern and temperature distribution suggests the interpolation method to improve using the results from the simulation.

INTRODUCTION

Slab reheating furnace is the first and one of the most important phase in the hot rolling process in steel industries. It is a precondition to heat the steel slabs above the recrystallization temperature before it can be mechanically treated to roll and make steel sheet. In the reheating furnace, fuel is combusted in air to produce very high temperature and the heating process of the steel slabs is governed mainly by the radiation from the turbulent flow and complex combustion. Normally, a reheating furnace is divided into different zones in order to reach a certain level of temperature to achieve a desired steel sheet quality. Most of the steel industries have their own recipe for a specific class of the steel sheet where they usually want to follow an ideal temperature curve through different zones in the furnace. In order to produce high grade steel sheet it is very important to

maintain the temperature level following the ideal curve. However, this is very challenging in reality since it is difficult to measure the steel slab surface temperature directly during furnace operation. Typically, during a normal furnace operation, the furnace wall temperature and the gas temperature profile are interpolated based on the gas temperature estimation and the measured temperatures from only few thermocouples in the respective zone. Then the wall and gas temperature is used as boundary conditions in the online tool to estimate the slab temperature to compare with the ideal curve and operate the furnace accordingly. It is rather seldom that the estimated slab temperature is fitted to the ideal curve at the beginning of the furnace at normal to high production rate. This is due to the way the furnace is controlled to maximize production and secure heating. However, there are lots of unknown factors as the interpolation method used in the online control tool does not consider the real and complex physics of the flow, combustion and the radiation associated to the furnace. By understating the underlying phenomena behind the combustion, it is possible to optimize the control of furnace operation while meeting the desired steel sheet properties. In this case, numerical simulations can complement the existing interpolation used in the online control tool by providing detail information about the flow and combustion.

The furnace is the biggest energy consumer in the hot rolling process, which directly influences the price of the steel sheets. A small amount of increased efficiency in the furnace will lead to a great amount of energy savings over time. The energy usage and emission policy in the country, environmental issues and the sustainability factors in the competitive market, insist them to investigate and upgrade the existing furnace structure. Therefore, in the recent years, it has been a great concern in the steel industries to investigate their furnace numerically to have better understanding of the ongoing phenomena behind the scene.

In recent years, researchers have been successfully modelling walking beam type reheating furnaces numerically [1-8]. A coupled numerical study was done in [1] to model a whole furnace in 3D where the authors reported that the numerical results agree reasonably well with the measurements, however disagreement was noticed for the slab surface temperature in the preheating zone. A simplified model was used in 2D in [2] to predict the heat flux through the slab surface where the

prediction from their model was consistent to the experimental data. In another investigation [3], a different approach called zonal division was used to model the furnace numerically in 3D. Two different models were used in their simulation where the first complete model served as input to the zonal model. The authors reported the zonal method to be faster than the full model while the accuracy of predicting temperatures at the same level as the full model. Similar type of zonal division approach was used to model the furnace in [4] by dividing the whole furnace into 14 sub-zones. The temperature of the zone wall and the medium was determined by the overall heat balance.

NOMENCLATURE

C_p	[J/(Kg.°C)]	Specific heat capacity
C	[-]	Constant
E	[J]	Total energy
f	[-]	Mixture fraction
\bar{f}	[-]	Mean mixture fraction
G_k	[-]	Generation of turbulence kinetic energy due to the mean velocity gradients
K	[W/(m.°C)]	Thermal conductivity
k	[m ² /s ²]	Turbulence kinetic energy
p	[Pa]	Pressure
Pr	[-]	Prandtl number
S	[J]	Source term
T	[°C]	Temperature
u	[m/s]	Velocity
u'	[m/s]	Fluctuating velocity
x	[m]	Cartesian axis direction
Y_M	[-]	Contribution of the fluctuating dilatation in compressible turbulence to the overall dissipation rate
Z_i	[-]	Elemental mass fraction for element i
Special characters		
δ_{ij}	[-]	Kronecker delta
ε	[m ² /s ³]	Turbulence dissipation rate
μ	[Kg/ms]	Dynamic viscosity
ν	[m ² /s]	Kinematic viscosity
ρ	[kg/m ³]	Density
τ_{ij}	[-]	Stress tensor
Subscripts		
ε		Turbulence dissipation rate
eff		Effective
$fuel$		Fuel stream inlet
h		Heat
k		Turbulence kinetic energy
m		Mass
μ		Dynamic viscosity
ox		Oxidizer stream inlet
t		Turbulent
$user$		User

A parametric analysis was done in [5] to investigate emissivity effect on the radiation heat transfer, where the importance of this parameter to predict the radiation correctly was discussed. An online numerical tool was developed to predict the radiative heat transfer without simulating the combustion in [6] and was validated by experiments with acceptable accuracy. A mathematical model was used in [7] to determine the optimal residence time in the furnace by comparing the heating characteristics of the slabs in different temperature of the furnace. The authors reported the influence of the slab residence time on energy consumption and pollutant

emission. An interesting investigation was done in [8] where they considered to model an adaptive system. In their model, a number of burners can be opened or closed based on the temperature response according to the heating curve to save energy. To identify the best combination they used a nonlinear least-square and pattern search method.

In all the previous investigations the furnaces are modelled using a very coarse mesh to get a rough overall flow and temperature distribution inside the furnace [1-8]. All the small scale details have been ignored in the above mentioned studies. The small scale features of turbulence and combustion chemistry may have significant effects on the combustion and radiation temperature. In this study, we model a single zone of the furnace in real scale and one burner of the same zone in detail to capture small scale features of the combustion and radiation. We analyse and visualize the flow field and temperature distribution inside the furnace. We have successfully compared the simulation results with measured data from the thermocouples. Moreover, we compare the slab temperature curve with the interpolated values collected from the online control system in the steel plant and with the ideal curve.

FURNACE AND BURNER CONFIGURATION

The studied furnace consists of 8 zones in total. Figure 1 shows a full furnace in 2D together with the burners' locations. In the present study, we focus only on Zone 1 of the furnace. Zone 1 has 8 burners in a line with capacity roughly 3500 KW each (Figure 2c). We model single burner in the middle among the 8 burners in Zone 1 together with a long slice of the furnace hall associated to Zone 1 (Figure 2b). The burners in Zone 1 are configured in a periodic manner, therefore the boundary conditions for the cross section surfaces on both sides of the numerical domain are used as periodic (Figure 2b). Zone 2 is having the power capacity almost similar to Zone 1. Therefore we assume Zone 2 to be identical with Zone 1 in our model and we use symmetry boundary condition to represent Zone 2 (Figure 2b). Wall boundary condition is used for the roof walls of the furnace. In the simulation the zones upstream from zone 1 and 2 is omitted due to unreasonably increased computational time when involving the whole furnace. The modelled system therefore involves a flow boundary at this imposed limit. The limit between Zone 1 and Zone 3 is modelled as a thin wall surface, where the gas temperature measured from the thermocouple was imposed as a uniform wall temperature boundary condition to get a realistic heat flux from Zone 3 to Zone 1.

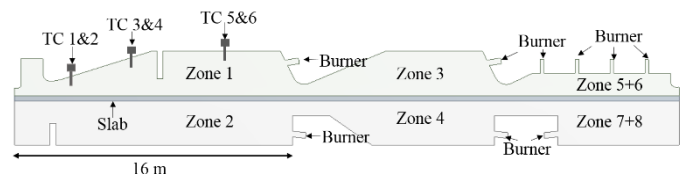


Figure 1 Whole furnace (side view) in 2D showing different zones, burners and thermocouples (TC) in Zone 1

The burner is having one air inlet and two gas lances for the LPG (C_3H_8). The gas lances are positioned in a way, so that they

are not aligned (Figure 2a, 2d), to get broader flame from the combustion.

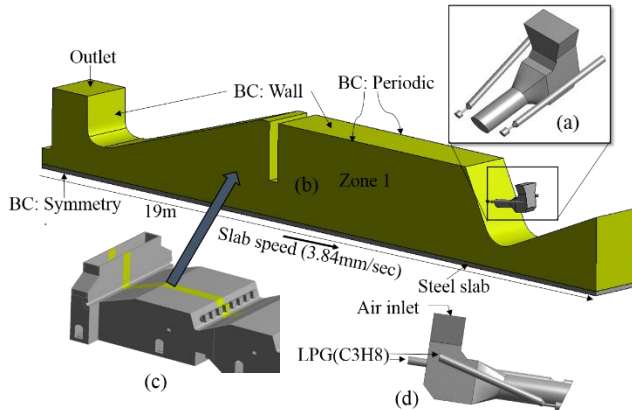


Figure 2 Numerical domain with boundary conditions (BC) (a) Burner configuration in 3D (b) Numerical domain with single burner (c) Zone 1 and 2 in 3D (d) Burner configuration in 2D

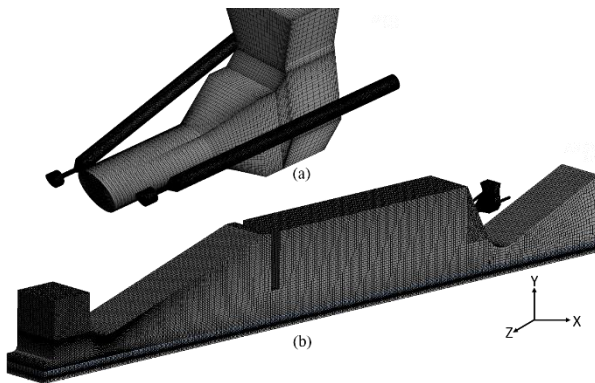


Figure 3 Mesh for the numerical domain (3.4 million cells) (a) burner (b) The whole domain

Figure 3 shows the mesh used for the simulation. Refined cells are used to capture the small scale details. The total number of elements in the mesh is about 3.4 million. The mesh y^+ values range is between 30 and 300. The y^+ resolution at the important slab surface is maintained at approximately 30. This y^+ range guaranties the turbulence wall law functionality.

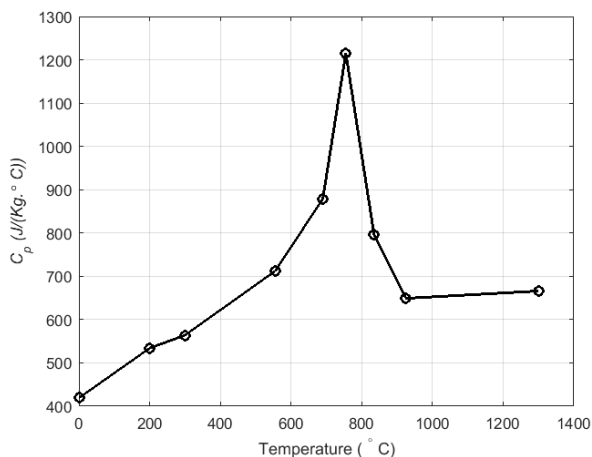


Figure 4 Specific heat (C_p) capacity of the steel slab

OPERATING CONDITIONS

During the furnace operation a single slab was tracked all the way in the furnace and the average data for the flow rates and thermocouple temperatures were obtained from the online control system. Moreover, the interpolated data from the thermocouples that are used to fit the ideal curve were also obtained from the online control tool. The air (21% O_2 and 79% N_2) flow rate in Zone 1 was $75200 \text{ m}^3/\text{hr}$ at 560°C inlet temperature and the LPG (C_3H_8) flow rate was $1000 \text{ m}^3/\text{hr}$ at 20°C inlet temperature. The reaction rate is assumed infinitely fast.

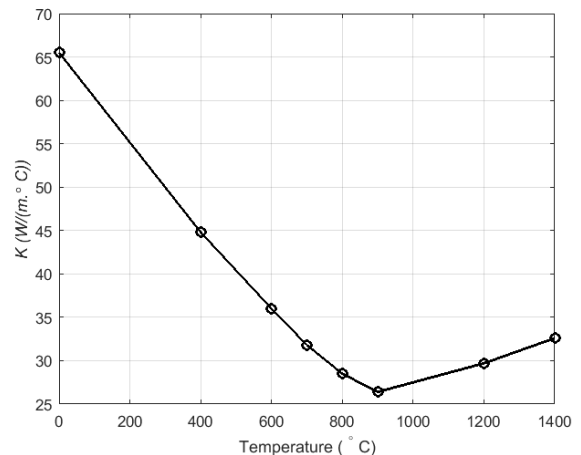


Figure 5 Thermal conductivity (K) of the steel slab

Since a single slab was tracked all the way during the furnace operation, instead of a number of discrete slabs, we consider a single continuous slab. This is a valid assumption since the distances between the slab pieces are very small. The slab in Zone 1 has a speed of 3.84 mm/sec . The material properties of the steel slab, the specific heat capacity as a function of temperature (Figure 4) and thermal conductivity as a function of temperature (Figure 5) are obtained from the steel plant. The density of the steel slab is set to 7488 kg/m^3 . The steel slab was modelled as opaque inside. The radiation absorption coefficient of the slab surface considered as 0.8. No radiation is modelled inside the steel slab. The walls of the air duct, the lances and the furnace roof is assumed to be adiabatic.

MATHEMATICAL MODELS

The computational system of transport equations, employed to model the furnace operation, involves solving the mass, the momentum and the energy transport equations. The turbulence is accounted for by using the Realizable $k-\epsilon$ turbulence model, which involves the transport equations for k and ϵ . The system is solved in steady state mode. Chemical reactions for combustion are included using the probability density function (PDF) method [9], commonly used for non-premixed combustion. In non-premixed combustion, the fuel and oxidizer enters into the combustion chamber separately. The mixing of the two streams must bring the reactants together in an efficient way for the reaction to be possible. The species involved in the reactions are: N_2 , O_2 , C_3H_8 , CHO , CO , CO_2 , H , H_2 , H_2O , H_2O_2 , HCO ,

HO₂, HOCO, O, OH, HONO, CH₄ and O₃. The radiation processes in the domain is modeled using the Discrete Ordinates (DO) Method [9]. In the simulation, the local species composition is used for evaluating the gas thermal radiation absorption coefficient. The gas is modeled using the grey gas assumption.

Mass and momentum transport equations:

The equation for conservation of mass employed is:

$$\frac{\partial}{\partial x_i}(\rho u_i) = 0$$

Conservation of momentum equation used for the simulations are:

$$\frac{\partial}{\partial x_j}(\rho u_i u_j) = -\frac{\partial p}{\partial x_i} + \frac{\partial}{\partial x_j} \tau_{ij} + \frac{\partial}{\partial x_j}(-\rho \overline{u'_i u'_j})$$

Where, the Newtonian fluid stress tensor,

$$\tau_{ij} = (\mu + \mu_t) \left(\frac{\partial u_i}{\partial x_j} + \frac{\partial u_j}{\partial x_i} - \frac{2}{3} \frac{\partial u_k}{\partial x_k} \delta_{ij} \right)$$

The Reynold stress term $(-\rho \overline{u'_i u'_j})$ is defined as:

$$-\rho \overline{u'_i u'_j} = \mu_t \left(\frac{\partial u_i}{\partial x_j} + \frac{\partial u_j}{\partial x_i} \right) - \frac{2}{3} (\rho k + \mu_t \frac{\partial u_k}{\partial x_k}) \delta_{ij}$$

Mixture fraction transport equation:

The mixture fraction concept can be utilized under the assumption of equal mass diffusivities of the species involved in the system. The individual species transport equation can then be reduced into a single transport equation for the mixture fraction, $f = \frac{Z_i - Z_{i,ox}}{Z_{i,fuel} - Z_{i,ox}}$.

$$\nabla \cdot (\rho \vec{v} \vec{f}) = \nabla \cdot \left(\frac{\mu + \mu_t}{\sigma_t} \nabla \vec{f} \right) + S_m + S_{user}$$

Where, μ and μ_t is laminar and turbulent viscosity respectively. σ_t is a constant with value 0.85.

Energy transport equation:

The energy transport together with the mass and momentum transport is described using the following equation:

$$\frac{\partial}{\partial x_i} [u_i (\rho E + p)] = \frac{\partial}{\partial x_j} \left(K_{eff} \frac{\partial T}{\partial x_j} + u_i (\tau_{ij})_{eff} \right) + S_h$$

Where E is the total energy, $K_{eff} = K + C_p \mu_t / Pr_t$ is the effective thermal conductivity, S_h is heat of the chemical reaction and $(\tau_{ij})_{eff}$ is the deviatoric stress tensor, defines as,

$$(\tau_{ij})_{eff} = \mu_{eff} \left(\frac{\partial u_i}{\partial x_j} + \frac{\partial u_j}{\partial x_i} \right) - \frac{2}{3} \mu_{eff} \frac{\partial u_k}{\partial x_k} \delta_{ij}$$

Turbulence model equations

The flow and the combustion inside the furnace is highly turbulent. To model the turbulence, Realizable $k - \varepsilon$ turbulence

model is used for the simulations. The equations for turbulent kinetic energy k and turbulent dissipation rate ε are as follows:

Turbulence kinetic energy transport equation:

$$\frac{\partial}{\partial x_j} (\rho k u_j) = \frac{\partial}{\partial x_j} \left[\left(\mu + \frac{\mu_t}{\sigma_k} \right) \frac{\partial k}{\partial x_j} \right] + G_k - \rho \varepsilon - Y_M$$

Turbulence dissipation rate transport equation:

$$\frac{\partial}{\partial x_j} (\rho \varepsilon u_j) = \frac{\partial}{\partial x_j} \left[\left(\mu + \frac{\mu_t}{\sigma_\varepsilon} \right) \frac{\partial \varepsilon}{\partial x_j} \right] + \rho C_1 S \varepsilon - \rho C_2 \frac{\varepsilon^2}{k + \sqrt{\nu \varepsilon}}$$

Where, turbulence viscosity: $\mu_t = \rho C_\mu \frac{k^2}{\varepsilon}$,

$$C_1 = \max \left[0.43, \frac{k}{\varepsilon} \frac{\sqrt{2 S_{ij} S_{ij}}}{\sqrt{2 S_{ij} S_{ij} + 5}} \right], C_2 = 1.9, \sigma_k = 1.0, \sigma_\varepsilon = 1.2$$

Gas mixture properties:

The gas density is modelled using the probability density function concept incorporated in the non-premixed combustion method. The gas mixture specific heat capacity, C_p is modelled using the mixing law [9]. The thermal conductivity, K of the gas is set to 0.0454 W/(m-K) and the molecular viscosity, μ , is set to 1.72e-5 Kg/(m-s).

RESULTS AND DISCUSSIONS

The flow and the combustion is highly turbulent inside the furnace and the 3D effects and mixing make it quite difficult to capture and visualize the interesting factors on 2D surfaces. Therefore, we present our results both on 2D and 3D surfaces to provide better understanding of the phenomena.

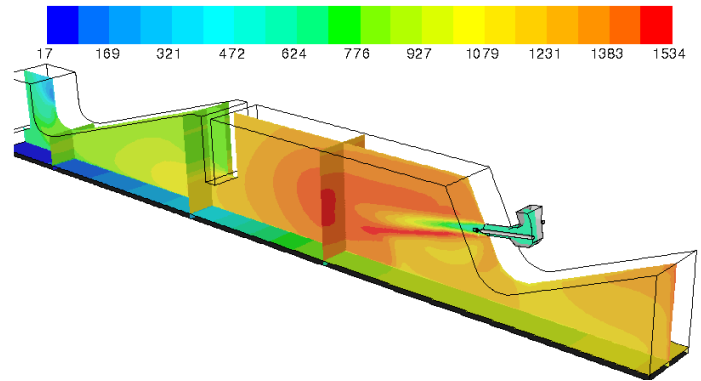


Figure 6 Temperature (°C) contour on cross section planes in the domain

We discuss the simulation results in this section based on temperature distribution and flow field. We compare the results with measured data to verify the accuracy of the simulation. Figure 6 shows the temperature contour on the cross section planes in the simulation domain.

As indicated before in Figure 1 that there are only 6 thermocouples in Zone 1 penetrating roughly 200 mm inside the furnace from the roof. Thermocouples 1&2 are aligned as shown in Figure 1. Similarly, thermocouples 3&4 and 5&6 are aligned.

The average data from each pair of thermocouples are obtained from the online control system tool and compared with the simulation data at the respective locations. The temperatures obtained from the simulation are in overall agreement with the measured temperature as shown in Table 1.

Table 1: Comparison between average temperature of thermocouples and simulation

	Average data TC 1 & 2 (°C)	Average data TC 3 & 4 (°C)	Average data TC 5 & 6 (°C)
Measurement	830 ± 2%	880 ± 2%	1320 ± 2%
Simulation	877	860	1310
Relative error	5.66%	2.27%	0.75%

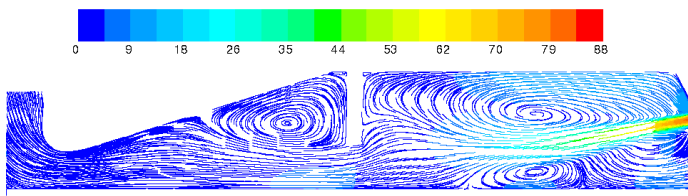


Figure 7 Path lines of the velocity (ms^{-1}) on the cross section plane in the middle of the domain showing the recirculation

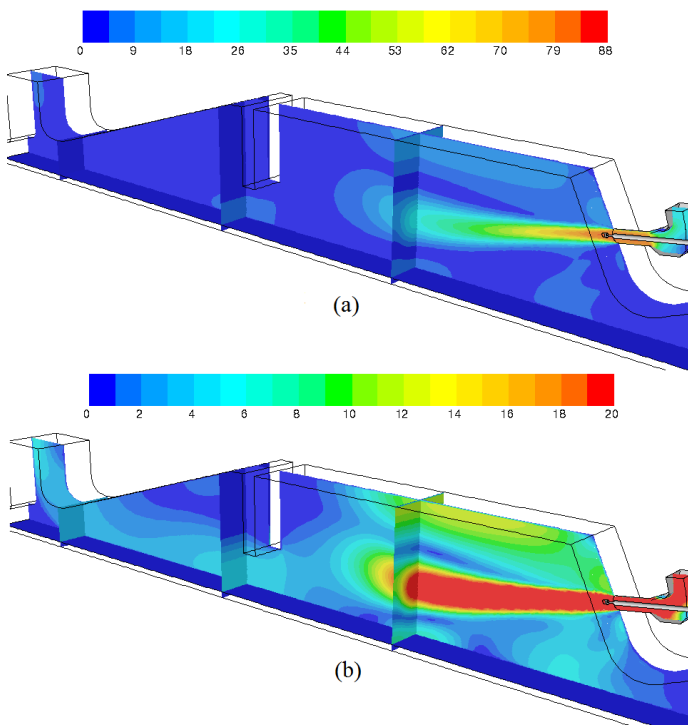


Figure 8 Velocity (ms^{-1}) contours on cross section planes in the domain (a) simulated maximum velocity range 0 – 88 ms^{-1} (b) simulated velocity range 0-88 ms^{-1} presented with color mapping 0 – 20 ms^{-1}

Figure 7 shows path lines of the velocity on the cross section plane in the middle of the simulation domain. High degrees of re-circulation are observed inside the furnace which causes a lots of mixing in the flow and combustion. Figure 8 illustrates the velocity contours on several cross section planes to visualize the velocity profile in 3D. Figure 8a presents the velocity ranged from 0 ms^{-1} to 88 ms^{-1} , which is the global range of velocity in the simulation domain. Figure 8b presents the velocity contour on the same planes as in Figure 8a but the color is mapped to 0 ms^{-1} to 20 ms^{-1} to highlight the lower velocity and visualize the overall flow pattern. In Figure 9, we compare the slab surface temperature from the simulation with the ideal curve and the interpolated data from the control system based on the measured temperatures. The interpolation is used to control the furnace to follow the ideal curve. However, the simulation shows somewhat different pattern of the slab surface temperature. It may be obvious to have this kind of shape of the curve from the simulation due to the steel properties. If we look at the specific heat capacity (Figure 4) and the thermal conductivity (Figure 5), a sharp increase in C_p and a steep decrease occurs roughly at 300°C. The slab surface temperature curve also gets sharp increase at around 300°C. The maxima of the specific heat capacity and the minima of the thermal conductivity exist in the temperature range of 750 to 1000°C, this has a strong influence on the slab surface temperature in the range of 10 to 14m slab length, as can be seen in Figure 9.

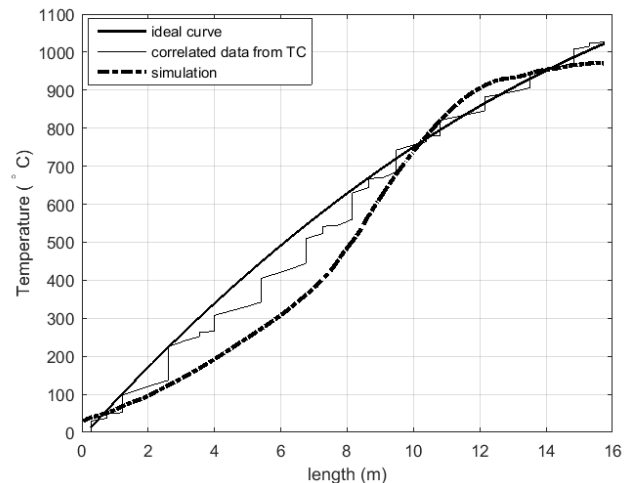


Figure 9 Surface temperature of the steel slab

The simulation (Figure 9) shows an overall good comparison with the ideal curve towards the end, however a significant underestimation is seen from the beginning until 10m length. The average temperature curve in the slab is presented in Figure 10. The curve with the interpolated measured temperatures is higher than the simulated curve. From previous investigation similar results for the volume average temperature is obtained in [3].

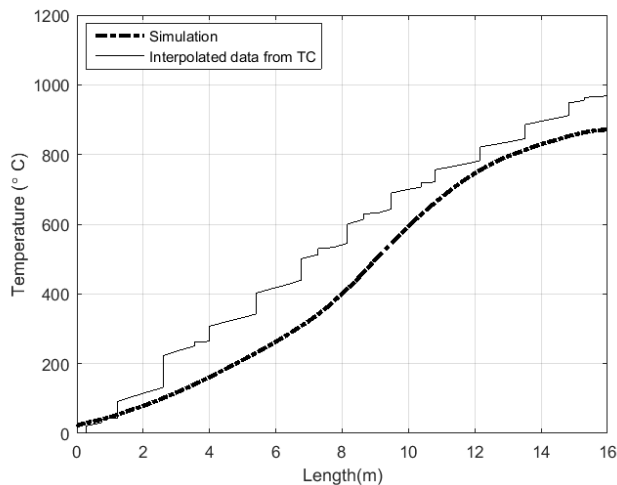


Figure 10 Volume average temperature of the steel slab

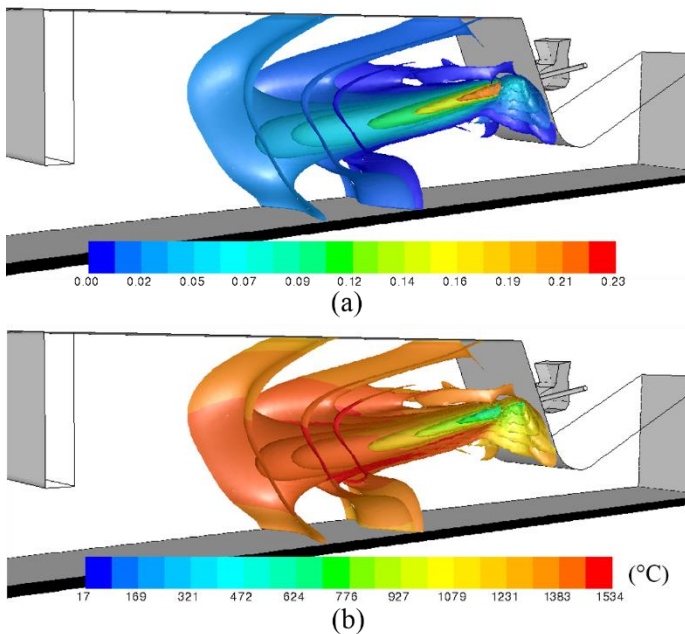


Figure 11 Iso surfaces (a) mass fraction of O_2 (b) temperature ($^{\circ}C$) on the iso-surfaces of mass fraction of O_2

Since the furnace is a heating process the slab surface temperature is higher than the slab core temperature which is shown in both measurements and simulation. The thermocouples positioned in the gas near the furnace roof is used for the evaluation of the slab average temperature. In order to transform the measured gas temperatures to a temperature in the slab solid in the online control system in the steel plant, an assumed heat transfer coefficient is used as well as a function for the thermal heat conduction in the slab. The interpolated slab temperature may therefore also be subject to the assumptions being made. It is therefore not fully clear how well the interpolation captures the phenomena behind the involved physics of the system, such as combustion, convection, conduction and thermal radiation?

Figure 11 shows 3D surfaces of different concentration of O_2 and the temperature on the same surfaces. The surfaces for lower O_2 concentration are like a horn shape. The lower the mass concentration (Figure 11a) of O_2 , the higher the combustion rate and the higher the temperature (Figure 11b).

Overall, the simulation predicts the gas temperature well (Table 1), however, the slab surface temperature and the average slab temperature from the simulation suggests to investigate and improve the interpolation method used in the control system in the steel industry.

CONCLUSION

The present work investigates the complex flow and combustion associated to the slab reheating furnace. The current study has successfully developed the model as a cross section of Zone 1, where the complete design of the burner is implemented and Zone 1 and Zone 2 is represented by simplification using boundary conditions. Our model has generally captured the involved recirculating turbulent flow in the furnace, overall producing the correct level of the gas temperature. However, disagreement is observed for the slab surface and slab average temperature when comparing with the interpolated data from the online control system. Our CFD model provides insight of the ongoing phenomena inside Zone 1 which can be used to complement or update the interpolation method used in the online control system.

The model can be refined by tuning different parameters, for example, absorption coefficient of the steel slab. The results of the simulation can also serve as input to the zonal method and make faster simulation to develop new tool for control in hot rolling steel industries.

ACKNOWLEDGEMENTS

The authors acknowledge the financial support for the project by SSAB and Mälardalen University, Sweden.

REFERENCES

- [1] Huang, M. J., Hsieh, C. T., Lee, S. T., & Wang, C. H. (2008). A coupled numerical study of slab temperature and gas temperature in the walking-beam-type slab reheating furnace. *Numerical Heat Transfer, Part A: Applications*, 54(6), 625-646.
- [2] Kim, M. Y. (2007). A heat transfer model for the analysis of transient heating of the slab in a direct-fired walking beam type reheating furnace. *International Journal of Heat and Mass Transfer*, 50(19), 3740-3748.
- [3] Morgado, T., Coelho, P. J., & Talukdar, P. (2015). Assessment of uniform temperature assumption in zoning on the numerical simulation of a walking beam reheating furnace. *Applied Thermal Engineering*, 76, 496-508.
- [4] Han, S. H., Chang, D., & Huh, C. (2011). Efficiency analysis of radiative slab heating in a walking-beam-type reheating furnace. *Energy*, 36(2), 1265-1272.
- [5] Harish, J., & Dutta, P. (2005). Heat transfer analysis of pusher type reheat furnace. *Ironmaking & steelmaking*, 32(2), 151-158.
- [6] Marino, P., Pignotti, A., & Solis, D. (2002). Numerical model of steel slab reheating in pusher furnaces. *Latin American applied research*, 32(3), 257-261.

- [7] Lee, D. E., & Kim, M. Y. (2013). Optimum residence time for steel productivity and energy saving in a hot rolled reheating furnace. *Journal of Mechanical Science and Technology*, 27(9), 2869-2877.
- [8] Srisertpol, J., Tantrairatn, S., Tragrunwong, P., & Khomphis, V. (2010, October). Temperature control for reheating furnace walking hearth type in heating curve up process. In *Proceedings of the 9th WSEAS international conference on System science and simulation in engineering* (pp. 464-469). *World Scientific and Engineering Academy and Society (WSEAS)*.
- [9] FLUENT theory guide and user manual, *ANSYS FLUENT 16.2*.